中國機械工程學刊第四十卷第一期第 1~10 頁(民國一百零八年)
Journal of the Chinese Society of Mechanical Engineers, Vol.40, No.1, pp 1~10 (2019)

CFD Simulation and Test of a High Pressure Piston Pump with Pre-Compression Chamber Structure

Xiao-Feng Wu*, Chih-Keng Chen**, Chih-Wei Hong***
and Wei Jiang*

Keywords： piston pump, flow ripple, CFD, PUMPLINX

ABSTRACT

Fluid noise in a piston pump is caused by pressure and flow ripples when the piston cavity rotates the pre-compression closed dead area of the valve plate. This paper studies a certain type of high pressure piston pump with pre-compression chamber. CFD simulations of the piston pump were carried out in PUMPLINX® and the results show that the flow ripple of piston pump is affected by the load pressure, pump speed and structure of the pre-compression chamber. DOE and approximate function technique are used to obtain the response surface function of flow ripple, which is expressed by structural parameters of the damping hole diameter and span angle of the pre-compression chamber. Damping hole diameter and span angle of the pre-compression chamber are optimized under different load pressures, based on the response surface function. After optimization, the outlet flow ripple rate is reduced under the load pressures of 100bar, 200bar and 300bar, respectively. Finally, piston pump flow rate test experiments are performed to verify the correctness of simulation.

INTRODUCTION

High pressure piston pump fluid noise caused by the piston pump outlet flow ripple is one of the important indicators to measure the performance of a pump. Because the piston cavity is alternately connected with the high and low pressure ports by the configuration flow mode, pressure mutation in the piston cavity results. This leads to outlet flow ripple of the piston pump, a phenomenon that is especially significant in high load conditions. In order to improve the performance of a high pressure piston pump by reducing fluid noise, flow ripple of the piston pump must be reduced. However, there are many factors affecting the outlet flow ripple of a piston pump, such as load pressure, rotation speed of the pump and structure of the valve plate transition zone. Analysis of flow ripple of the piston pump and methods of reducing it have been studied by many researchers.

Edge and Harrison (Edge, E. A., 1983; Harrison, K., 2002) studied the theory of fluid pressure and flow characteristics in piston pumps and developed a theoretical model for flow ripple of a piston pump outlet, although the effect of leakage in the piston pump was not considered. Manring (Manring, N. D., 2000 and 2003) studied performance of the piston pump including the effects of a damping hole in the valve plate, developed an actual flow model of the piston pump outlet and analyzed the effect of the damping hole on the volume efficiency. Mandal (2008) studied the fluid characteristics of a piston pump with a sinking groove structure on the valve plate and analyzed the effect of the groove structure on flow ripple of the piston pump outlet. Yang and Xu (2010) studied the internal flow characteristics and the CFD simulation of a piston pump, proposing a drive design method for a piston pump valve plate with a hole and groove combined. This combined hole and groove structure was optimized under the goal of minimum flow ripple in a piston pump correctness of the simulation was experimentally verified. Yin and Nie (2015) studied effects of the valve plate pre-loading angle on outlet flow ripple in an axial piston pump. Wang and Wu (2011 and 2014) studied the CFD simulation of a piston pump and analyzed the effect of a valve plate triangular groove on the outlet flow ripple of a piston pump.Chihkeng Chen and Xiaofeng Wu studied the structural parametric design of a piston pump and analyzed the effect of valve plate structure parameters

Paper Received, October, 2018. Revised December, 2018. Accepted December, 2018. Author for Correspondence: Chih-Keng Chen.

* *Associate Professor, School of Mechanical and Vehicle Engineering, Changzhou Institute of Technology, China*

** *Associate Professor, Department of Vehicle Engineering, National Taipei University of Technology, Taiwan*

*** *Engineer, YEOSHE Hydraulic Co., LTD, Taiwan*

on flow ripple of piston pump (2017)

All these previous studies analyzed the influence on fluid characteristics of piston pump valve plate structure in a piston pump and flow ripple based on CFD model simulations. Most of the researches have been on valve plates with a triangular or U-shaped groove. Pre-compression in a piston cavity can be realized by the design and optimization of a triangular or U-shaped groove that can reduce the flow ripple of the piston chamber pressure fluctuations and exports. However, there has been very limited research on piston pumps with a pre-compression chamber. Accordingly, this article considers the piston pump with a pre-compression chamber and uses PUMPLINX® software to explore CFD simulation, thereby analyzing the influence of diameter of damping hole of pre-compression, span of damping hole and volume of pre-compression on flow ripple of a piston pump.

The YEOSHE PV270 piston pump from YEOSHE Hydraulic Co.,LTD is used as the study object, as shown in Fig.1. This includes 9 pistons, and power is transferred from the main shaft to the cylinder block, which drives the pistons' rotation. The piston head is covered with a slipper that is close to the face of swash plate. With the circular motion of piston around the drive shaft, the piston also has a linear motion along the hole of cylinder block, so the volume of the piston cavity changes periodically. The piston cavity discharges oil when it is connected to the oil discharge chamber through the valve plate, and it sucks oil when it connected to the oil suction chamber through the valve plate.

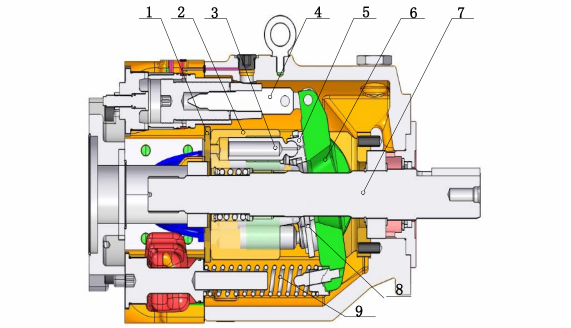

1-Valve plate; 2-Cylinder block; 3-Piston; 4-Inclination mechanism;5-Slipper; 6-Swash plate; 7-Drive shaft; 8-Return plate; 9-Angle adjust spring.
Fig. 1. The structure diagram of axial piston pump.

The YEOSHE PV270 type piston pump has a pre-compression chamber located between the oil suction chamber and oil discharge chamber, as shown in Fig.2. When the piston cavity rotates from the oil suction chamber in order to avoid hydraulic shock and back flow from the piston cavity, the piston cavity needs to be pre-compressed. Commonly used methods for this pre-compression are a triangular or U-shaped groove on the valve plate between the oil suction chamber and oil discharge chamber. In this paper, the piston cavity is connected to the pre-compression chamber to achieve the pre-compressing and pre-loading (Kumar S. J. et. al., 2009; Manring, N. D., 2001).

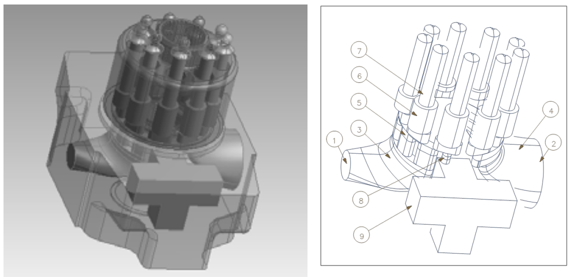

1-Discharge oil outlet, 2-Suction oil inlet,3-Discharge oil chamber,4-Suction oil chamber,5-Valve plate, 6-Cylinder bore,7-Piston cavity,8-Pre-compression damping hole,9-Pre-compression chamber.
Fig. 2. Flow channel and fluid structure of the pump.

THEORETICAL ANALYSIS AND CFD EQUATIONS

When the piston is located on the top dead center position of the valve plate, as shown in Fig.3, the piston rotation angle is defined as 0 degrees, and the displacement of the piston relative to the piston cavity is shown in Eq. 1.

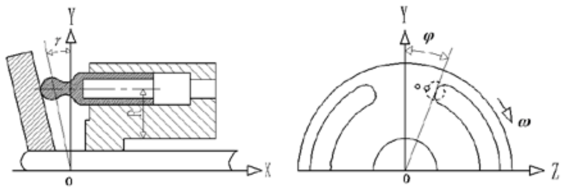

Fig. 3. Sketch diagram of piston motion

$$X = -R \cdot \cos\varphi \cdot \tan\gamma \tag{1}$$

In the Eq.1, X is the displacement of piston relative to piston cavity; R is the circular radius of the cylinder bore; φ is the piston rotation angle; γ is the inclination angle of the swash plate. Therefore, the speed of the piston relative to piston cavity is expressed as Eq.2.

$$v = R \cdot \omega \cdot \tan\gamma \cdot \sin\varphi \tag{2}$$

For this piston pump, the pump rotation speed $n = 1500rpm$; $R = 62.5mm$; $\gamma = 18.6°$; $\omega = 2\pi n / 60$. The specific function of the piston speed is shown in Eq.3.

$$v = 3.3023 \sin 157t \tag{3}$$

According to the Eq.1 to Eq.3, the instantaneous flow rate of single piston cavity is obtained as Eq.4.

$$q_i = \frac{\pi d^2}{4} \cdot v = \frac{\pi d^2}{4} R\omega \tan\gamma \sin\varphi_i \tag{4}$$

In Eq.4, d is the piston diameter, $d = 31mm$; q_i is the instantaneous flow rate of the first piston cavity from the top dead center of valve plate; φ_i is the instantaneous piston rotation angle of the i piston cavity. The instantaneous theoretical flow rate of the whole piston pump is obtained as Eq.5.

$$Q = \frac{\pi d^2}{4} R\omega \tan\gamma \sum_{i}^{m} \sin[\varphi_1 + 2(i-1)\beta] \tag{5}$$

In Eq.5, φ_1 is the angle of piston cavity which is nearest to top dead center in the oil discharge area; $2\beta = 360° / z$, z is the total number of piston cavities, $z = 9$; m is the number of piston cavities that are in the oil discharging state. When the $0 \le \varphi_1 \le \beta$, $m = 1/[2(z+1)]$; when the $\beta \le \varphi_1 \le 2\beta$, $m = 1/[2(z-1)]$. By analysis, when the $\varphi_1 = \beta/2$, the instantaneous flow rate of piston pump reaches maximum, $m = 5$; when the $\varphi_1 = 0$ or $\varphi_1 = \beta$; the instantaneous flow rate of piston pump is minimum, $m = 4$. Therefore, the maximum instantaneous flow rate Q_{max}, the minimum instantaneous flow rate Q_{min} and the average instantaneous flow rate Q_{ave} are obtained from Eq.6,Eq.7 and Eq.8.

$$\begin{aligned} Q_{max} &= \frac{\pi d^2}{4} R\omega \tan\gamma \sum_{i=1}^{5} \sin[\frac{\beta}{2} + 2\beta(i-1)] \\ &= 2.49 \times 10^{-3} \times \sum_{i=1}^{5} \sin[\frac{20°}{2} + 40° \times (i-1)] \\ &= 430.386 L/\min \end{aligned} \tag{6}$$

$$\begin{aligned} Q_{min} &= \frac{\pi d^2}{4} R\omega \tan\gamma \sum_{i=1}^{4} \sin[0 + 2\beta(i-1)] \\ &= 2.49 \times 10^{-3} \times \sum_{i=1}^{4} \sin[0 + 40° \times (i-1)] \\ &= 423.840 L/\min \end{aligned} \tag{7}$$

$$\begin{aligned} Q_{ave} &= \frac{\pi d^2}{4} z \times 2R \tan\gamma \cdot \frac{\omega}{2\pi} \\ &= \frac{157 \times 31^2}{4} \times 9 \times 62.5 \times \tan 18.6° \\ &= 428.424 L/\min \end{aligned} \tag{8}$$

The theoretical flow ripple of piston pump outlet is obtained as shown in Eq.9.

$$\delta_t = \frac{Q_{max} - Q_{min}}{Q_{ave}} = \frac{6.546}{428.424} = 1.528\% \tag{9}$$

According to the theoretical instantaneous flow calculation of the piston pump, it can be found that the average flow rate of piston pump is about 428 $L/\min$, and the flow ripple rate is about 1.526% obtained from Eq.9. However, the actual situation is not so, because the theoretical calculation of flow rate completely ignores the compressibility of the fluid which leads to reverse flow and fluid impact in piston cavity, this is the main reason for the flow ripple of the piston pump. The actual flow ripple rate is over ten times higher than the theoretical flow ripple rate, and it also affected by the pump external load pressure, pump speed, valve plate structure and other factors. In this paper, based on the theoretical calculation results, the actual flow simulation of piston pump is simulated by PUMPLINX®

The computational fluid dynamics equations in PUMPLINX® are as follows.

Continuity Equation:

$$\frac{\partial \rho}{\partial t} + \nabla \cdot (\rho u_i) = 0 \tag{10}$$

In Eq.10, ρ is the fluid density; ∇ is the differential operator for each direction; and u_i is the fluid velocity of direction i.

Momentum Equation:

$$\rho \frac{\partial u_i}{\partial t} + \rho u_j \frac{\partial u_i}{\partial x_j} = \rho F_i - \frac{\partial p}{\partial x_i} + \mu \frac{\partial^2 u_i}{\partial x_i x_j} \tag{11}$$

In Eq.11, u_i and u_j are fluid velocities of the i and j directions, respectively; x_i and x_j are direction vectors for the i and j directions, respectively; F_i is the external force in the i direction; p is the fluid pressure; μ is the dynamic viscosity.

Standard $K-\varepsilon$ Equation:

$$\rho\left(\frac{\partial K}{\partial t} + u_j \frac{\partial K}{\partial x_j}\right) = \frac{\partial}{\partial x_j}\left[\left(\mu + \frac{\mu_t}{\sigma_k}\right)\frac{\partial K}{\partial x_j}\right] + G_k - \rho\varepsilon \tag{12}$$

$$\rho\left(\frac{\partial \varepsilon}{\partial t} + u_j \frac{\partial \varepsilon}{\partial x_j}\right) = \frac{\partial}{\partial x_j}\left[\left(\mu + \frac{\mu_t}{\sigma_\varepsilon}\right)\frac{\partial \varepsilon}{\partial x_j}\right] + C_{\varepsilon 1}\frac{\varepsilon}{K} G_k - C_{\varepsilon 2}\rho\frac{\varepsilon^2}{K} \tag{13}$$

In Eq.12 and Eq.13, K is the turbulent kinetic energy; ε is the turbulent dissipation rate; μ_t is the coefficient of eddy viscosity; G_k is the turbulent kinetic energy generated by the mean velocity gradient; σ_k and σ_ε are the Prandtl coefficients for $\sigma_k = 1.0$, $\sigma_\varepsilon = 1.3$, respectively; $C_{\varepsilon 1}$ and $C_{\varepsilon 2}$ are constant coefficients, with $C_{\varepsilon 1} = 1.44$ and $C_{\varepsilon 2} = 1.92$.

CFD SIMULATION ANALYSIS

Piston Pump Fluid Model

The three dimensional fluid model of piston pump is developed by UG and imported into PUMPLINX®. The swash plate center is defined as [0, 0.16578, 0] and its unit is m; and the swash plate normal is set to [0, 3, -1] , which defines the inclination angle of swash plate to be 18.6°. Rotation speed of the piston pump is set to 1500 rpm. The Swash Plate Piston Pump template is used to generate the 9 pistons' mesh models of the piston pump, and the maximum and minimum mesh grid are respectively set to 0.025m and 0.001m. The General Mesh template is used to generate the other mesh models of the piston pump, and the maximum and minimum mesh grid are also set to 0.025m and 0.001m. The final piton pump mesh grid model is shown in Fig.4.

Fig. 4. Mesh grid model of a piston pump.

Simulation Results

The piston cavity is first connected with the pre-compression chamber when it rotates out of the oil suction zone, with the pressure distribution as shown in Fig.5(a). At this point, the fluid pressure in the pre-compression chamber is higher than the pressure in the piston cavity and the fluid flows into the cavity. Pressure of the pre-compression chamber then decreases and pressure in the piston cavity rises rapidly because of the increased flow and compression. As shown in Fig.5(b), when the piston cavity connects to the oil discharge chamber, there will be a sudden hydraulic shock because of excessive pre-compression or a back flow from oil discharge chamber due to inadequate pre-compression in the piston cavity, as shown in Fig.6. The pre-compression chamber supplements the pressure and acts as a buffer, When the piston cavity is just connected with the pre-compressed chamber, the pressure of the pre-compressed chamber decreases, and when the piston cavity and the outlet cavity are connected, the pressure of the outlet cavity is higher than that of the piston cavity and the pre-compressed chamber, and the oil will flow back from the outlet cavity to the pre-compressed cavity, thus the pre-compressed cavity will be compensated, so in the pre-compression chamber the pressure presents a cyclical change of around 130 bar, as also shown in Fig.6 (Paolo, C. et. al., 2006; DING, H. et. al., 2011).

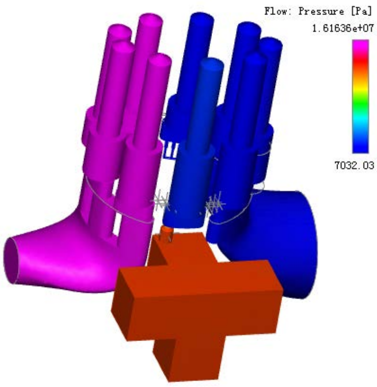

(a)

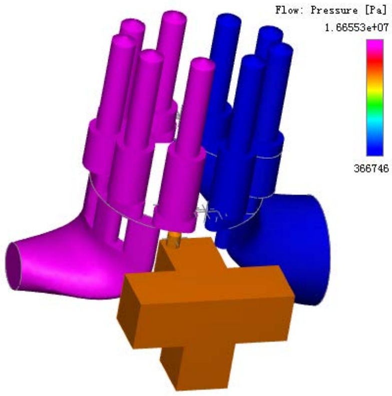

(b)

Fig. 5. Pressure distribution in piston pump

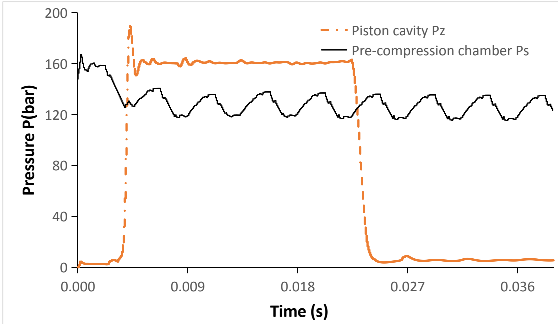

Fig.6. Pressure change in the piston cavity and pre-compression chamber

Effect of Load Pressure on Flow Ripple

In order to analyze the influence of different load pressures on the PV270 piston pump flow ripple, the pump outlet pressures are set to 100bar, 200bar and 300bar, in the simulations. The PV270 piston pump flow rate change curve is shown in Fig.7. According to the calculation of the maximum flow rate, minimum flow rate and average flow, the flow ripple rate is obtained as shown in Tab.1.

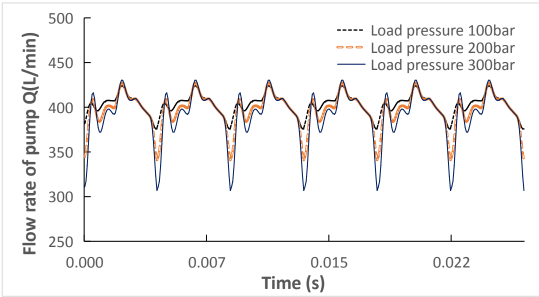

Fig.7. Flow rate under different load pressures.

Tab.1. Flow ripple under different load pressure.

Load (bar)	Q_{max} (L/min)	Q_{min} (L/min)	Q_{ave} (L/min)	Δ (L/min)	$\delta = \Delta / Q_{ave}$ (%)
100	423.86	375.76	402.75	48.10	11.94
200	427.29	340.90	396.81	86.39	21.77
300	430.20	306.81	391.60	123.39	31.51

Combining Fig.7 and Tab.1, the flow ripple rate of piston pump can be seen to rise from 11.94% to 21.77% and to 31.51% when piston pump outlet pressure changes from 100bar to 200bar and to

300bar. The change of maximum flow rate is weak when the load pressure continues to rise, but the change of minimum flow rate is severe as shown by comparison of the data in Tab.1. Larger load pressure leads to greater difference between the piston cavity and the oil discharge chamber when piston cavity connects with the oil pressure chamber. This causes back flow from the oil discharge chamber to the piston cavity and the flow ripple ratio becomes increases.

Effect of Pump Speed on Flow Ripple

The pump speeds are set to 1000rpm, 1500rpm and 2000rpm, respectively, in the simulation model and the corresponding piston pump outlet flow curves are shown in Fig.8.

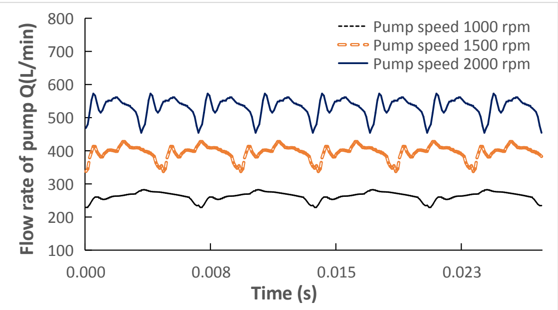

Fig.8. Flow rate of the piston pump under different pump speeds.

Tab.2. Flow ripple under different pump speeds

Pump Speed (rpm)	Q_{max} (L/min)	Q_{min} (L/min)	Q_{ave} (L/min)	Δ (L/min)	$\delta = \Delta / Q_{ave}$ (%)
1000	282.46	229.10	263.41	53.36	20.26
1500	427.56	337.59	394.66	89.97	22.80
2000	572.71	454.24	531.51	118.47	22.28

As shown in Fig.8 and Tab.2, when the pump speed increases from 1000rpm to 1500rpm, average flow rate of the piston pump increases by 263.41L/min to 394.66L/min, and flow ripple ratio increases from 20.26% to 22.80%. When the pump speed increases from 1500rpm to 2000rpm, average flow rate of the piston pump increases by 394.66L/min to 531.5L/min, but the flow ripple ratio drops from 22.80% to 22.28%. Simulation data shows that when the pump speed increased from 1000rpm to 1500rpm, there will be a maximum flow ripple ratio value, and as the pump speed continue to increase, the flow ripple ratio will fall.

Effect of Valve Plate Structure on Flow Ripple

Many studies have shown that a triangular groove, a damping hole and a U-shaped groove on the valve plate can reduce flow ripple of the piston pump outlet. The research object of this paper, the YEOSHE PV270 type piston pump, depends on a pre-compression chamber structure for pre-compression and on a buffer to reduce flow ripple of the piston pump outlet. Fig.9 shows the structure of the piston pump’s valve plate, diameter of the damping hole, volume of the pre-compression chamber and span of the damping hole. These are parameterized, and the parameter definitions are shown in Tab.3. Simulation is used to analyze the influence of three parameters of pre-compression chamber on the flow ripple of piston pump outlet.

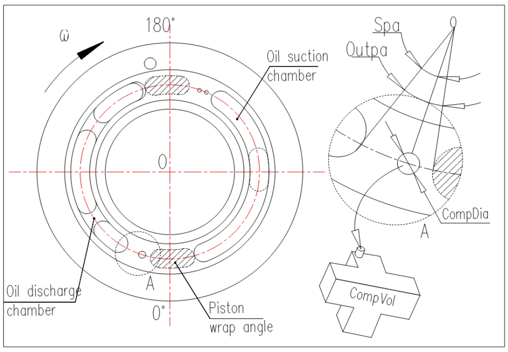

Fig.9. Structure of valve plate in the piston pump.

Tab.3. Valve plate structure parameters.

Parameters	Description
CompDia	Diameter of damping hole communicated with pre-compression chamber
CompVol	Volume of pre-compression chamber
Spa	Damping hole span of pre-compression zone

With the *CompDia* set to 2mm, 3.5mm and 5mm, simulation is carried out and its flow rate curves are shown in Fig.10.

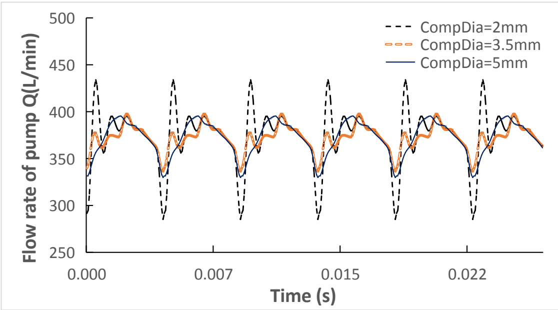

Fig.10. Flow rate under different diameters of damping hole

Tab.4. Flow ripple under different diameters of damping hole

CompDia (mm)	Q_{max} (L/min)	Q_{min} (L/min)	Q_{ave} (L/min)	Δ (L/min)	Δ / Q_{ave} (%)
2	433.99	285.15	373.36	148.84	39.87
3.5	397.51	336.47	371.60	61.05	16.43
5	395.38	329.78	371.27	65.60	17.67

There is a great difference in outlet flow rate of the piston pump with different damping hole diameters. After calculation and comparison, the results are listed in Tab.4. When the damping hole diameter is too small, this will cause very large flow ripple. When the damping hole diameter increases from 2mm to 3.5mm, the flow ripple ratio decreases from 39.87% to 16.43% because the smaller damping hole is difficult to buffer and compress. If the piston cavity is not pre-compressed enough, there is still a large pressure difference between piston cavity and oil discharge chamber when the piston cavity connects to the oil discharge chamber. This causes back flow from oil discharge chamber to piston cavity, which leads to substantial reduction in flow rate of the piston pump outlet. When the damping hole diameter increases from 3.5mm to 5mm, the flow ripple ratio increases from 16.43% to 17.67%, the minimum flow rate of piston pump outlet declines, and the flow ripple ratio increases. This is because a larger damping hole diameter leads to greater back flow from oil discharge chamber to pre-compression chamber, and the minimum flow rate from piston cavity to oil discharge chamber is smaller. Therefore, the damping hole diameter should be designed properly.

With the $CompVol$ set to 300cm^3, 600cm^3 and 900cm^3, the simulation is carried out and the flow rate curves are shown in Fig.11.

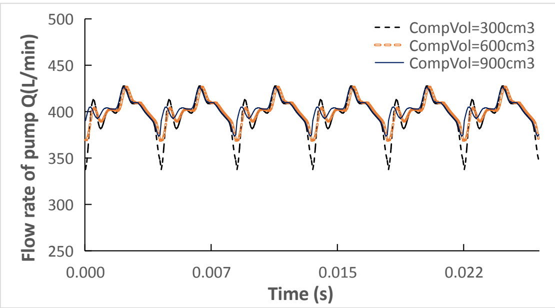

Fig.11. Flow rate under different pre-compression chamber volumes.

Tab.5. Flow ripple ratio under different pre-compression chamber volumes.

$CompVol$ (cm3)	Q_{max} (L/min)	Q_{min} (L/min)	Q_{ave} (L/min)	Δ (L/min)	Δ / Q_{ave} (%)
300	427.56	337.59	396.91	89.97	22.67
600	426.49	368.82	400.19	57.68	14.41
900	425.87	373.34	402.06	52.53	13.07

The function of pre-compression chamber is to fill the piston cavity in order to increase the pressure before the piston cavity connects with the oil discharge chamber. The flow ripple ratio is calculated in Tab.5. When the pre-compression volume is 300cm^3, the flow ripple ratio is close to 22.67%. When the pre-compression volume increases from 300cm^3 to 600cm^3, the flow ripple ratio declines from 22.67% to 14.41% because a larger pre-compression volume leads to more powerful buffering and compressing. When the pre-compression volume increases from 600cm^3 to 900cm^3, the flow ripple ratio declines from 14.41% to 13.07%, indicating that the pre-compression chamber is sufficient to achieve buffering and pre compressing with a volume of about 600cm^3. As the pre-compression volume continues to increase, the flow ripple of piston pump outlet declines only slightly.

With the Spa set to 5°, 7°and 9°, flow rate of the PV270 piston pump is obtained by simulation, and the flow rate curves are shown in Fig.12.

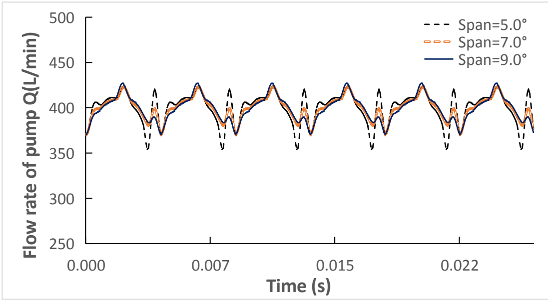

Fig.12. Flow rate under different span angles of damping hole.

Tab.6. Flow ripple ratio under different span angles of damping hole.

Spa (°)	Q_{max} (L/min)	Q_{min} (L/min)	Q_{ave} (L/min)	Δ (L/min)	Δ / Q_{ave} (%)
5	424.25	354.06	399.80	70.20	17.56
7	423.19	370.40	399.59	52.78	13.21
9	426.90	370.45	399.11	56.45	14.15

By calculation, the flow ripple ratios are obtained as shown in Tab.6. When the damping hole span angle increases from 5°to 7°, and the flow ripple ratio of the piston pump outlet is reduced from 17.56% to 13.21%. When the damping hole span angle continues to increase from 7°to 9°, the flow ripple ratio of the piston pump outlet increases from 13.21% to 14.15%. According to these results, if the damping hole span angle is smaller, the piston cavity pre-compression time is longer, which produces hydraulic shock; and when there is a higher instantaneous flow rate of piston pumping out, this leads to an increase of the flow ripple ratio. Conversely, if the damping hole span angle is larger, the piston cavity has a shorter pre-compression time, which produces back flow from oil discharge chamber to piston cavity, and this phenomenon also causes the increased flow ripple ratio of the piston pump outlet.

OPTIMIZATION

DOE and Approximate Modeling

The simulation results show that the outlet flow ripple rate is affected by uncontrollable factors such as load pressure and pump speed, the impact of load pressure is larger, and the impact of pump speed is very small so it can be ignored. Furthermore, the flow ripple rate is also affected by the structure of the pre-compression chamber, when the damping hole diameter and damping hole span angle change from small to large in the setting interval, the flow ripple rate will present a minimum value in the interval. When the volume of the pre-compression chamber changes from small to large, the flow ripple rate will continue to decrease, since the volume change of pre-compression chamber has little effect on the flow ripple rate when the volume of the pre-compression chamber is larger than 500cm3. This shows that the volume of pre-compression chamber is more than 500 cm3 to meet the requirements under the conditions permitted.

Based on above conclusions, in order to minimize the outlet flow ripple rate of the piston pump, the damping hole diameter and damping hole span angle of the pre-compression chamber should be optimized under the different load pressures. The DOE is conducted based on the full factors method, while the damping hole diameter and damping hole span angle are used as the design variables and the flow ripple rate is used as the target, the results of DOE are shown in Tab.7.

Tab.7. DOE analysis of outlet flow ripple rate based on full factors method.

Load P_o (bar)	Damping hole diameter $CompDia$ (mm) (x_1)	Damping hole span angle Spa (°) (x_2)	Outlet flow ripple rate δ (%) (y)
100	2	5	23.45
	2	7	21.06
	2	9	22.18
	3.5	5	12.03
	3.5	7	9.54
	3.5	9	10.01
	5	5	13.13
	5	7	10.42
	5	9	14.76
200	2	5	32.65
	2	7	26.44
	2	9	28.32
	3.5	5	18.22
	3.5	7	16.65
	3.5	9	21.46
	5	5	18.91
	5	7	17.83
	5	9	22.52
300	2	5	40.37
	2	7	34.88
	2	9	36.67
	3.5	5	26.14
	3.5	7	19.27
	3.5	9	21.68
	5	5	29.77
	5	7	22.93
	5	9	26.69

Based on the DOE data shown in Tab.7, the response surface function method and the response surface function error decision model is conducted in Eq.14 and Eq.15. The second order response surface function models are obtained in Tab.8 when the load pressure is 100bar, 200bar and 300bar. Charts of the response surface are shown in Fig.13.

$$y = \beta_0 + \sum_i \beta_i x_i + \sum_i \beta_i x_i^2 + \sum_{i \neq j} \beta_{ij} x_i x_j \tag{14}$$

$$R^2 = 1 - \frac{\sum_{j=1}^{N} [y_{rsm}(j) - y(j)]^2}{\sum_{j=1}^{N} [y(j) - \bar{y}]^2} \tag{15}$$

In Eq.14 and Eq.15, y_{rsm} and $y(j)$ are the response value and simulation value, respectively; $\bar{y}$ is the simulation average value; N is the inspection points; β_i is the weighted coefficient.

Tab.8. Approximate response surface function of flow ripple.

Load (bar)	Approximate response surface function of flow ripple	Inspection coefficient
100	$y_1 = 3.099x_1^2 + 0.563x_2^2 + 0.242x_1x_2 - 26.540x_1 - 8.871x_2 + 92.52$	$R_1^2 = 0.984$
200	$y_2 = 2.519x_1^2 + 0.843x_2^2 + 0.662x_1x_2 - 25.394x_1 - 13.913x_2 + 114.4$	$R_2^2 = 0.965$
300	$y_3 = 4.232x_1^2 + 1.132x_2^2 + 0.052x_1x_2 - 33.60x_1 - 16.961x_2 + 147.11$	$R_3^2 = 0.922$

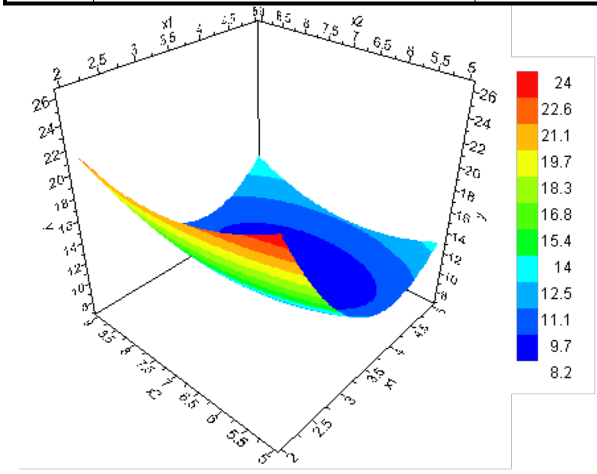

(a) 100bar

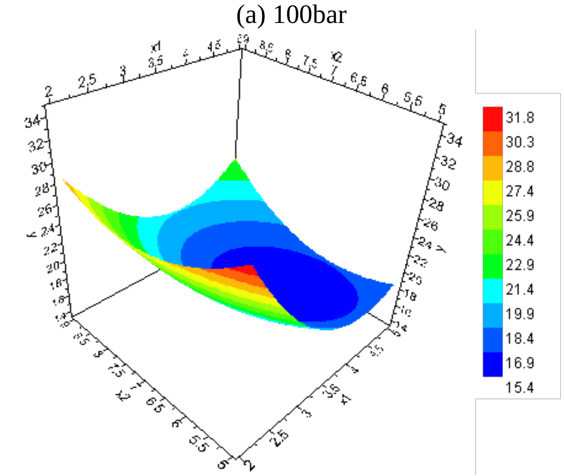

(b) 200bar

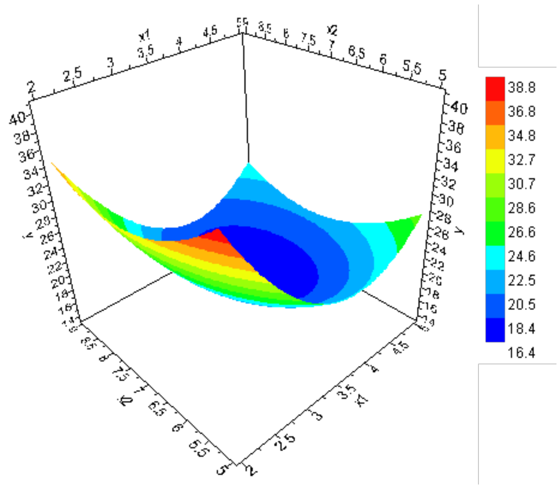

(c) 300bar

Fig.13. Flow ripple response surface under different load pressures.

Optimization Results

In order to minimize the outlet flow ripple rate under the different load pressures, the objective functions are developed as Eq.16 (Guan, C. B. et. al., 2013).

$$\begin{cases} objective1: \min(y_1) \\ objective2: \min(y_2) \\ objective3: \min(y_3) \\ constraints: 2 \le x_1 \le 5; 5 \le x_2 \le 9 \end{cases} \tag{16}$$

After multi-objective optimization, when the damping hole diameter is 3.994mm and the damping hole span angle is 7.074°, the minimum flow ripple rate are obtained under the load pressure of 100bar, 200bar and 300bar which are shown in Tab.9.

Tab.9. Structural parameters and flow ripple ratio before and after optimization

	x_1 (mm)	x_2 (°)	y_1 (%)	y_2 (%)	y_3 (%)
Before optimization	3	9	11.94	21.77	31.51
After optimization	3.99	7.07	8.21	15.63	18.56

EXPERIMENT

In order to verify the correctness of the simulation data and the optimization data, a piston pump flow rate test platform is developed, where the outlet flow rate of piston pump is measured under different load pressures. The test bench is shown in Fig.14 and the principle of the test experiment is shown in Fig.15. An LT1600 turbine flow meter is used for flow measurement, Compact DAQ is used for data acquisition and LABVIEW is used as the computer platform.

(a) Flow test bench

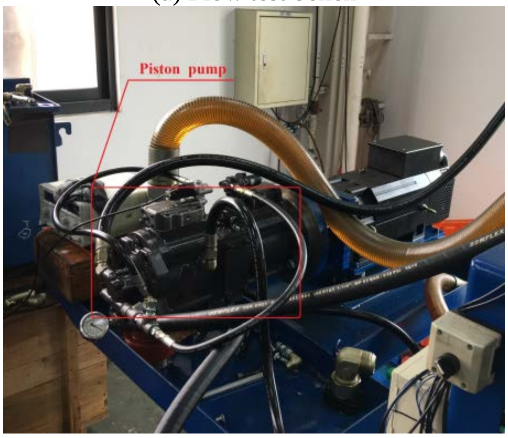

(b) Piston pump in experiment

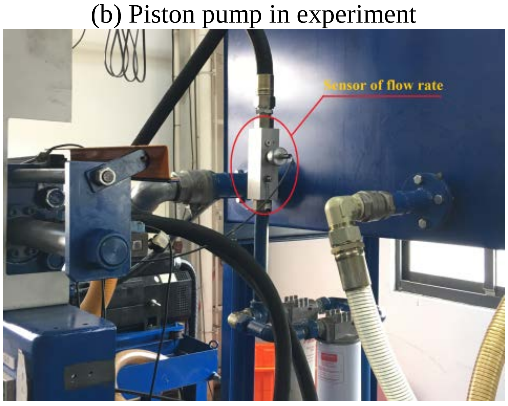

(c) Flow sensor in experiment

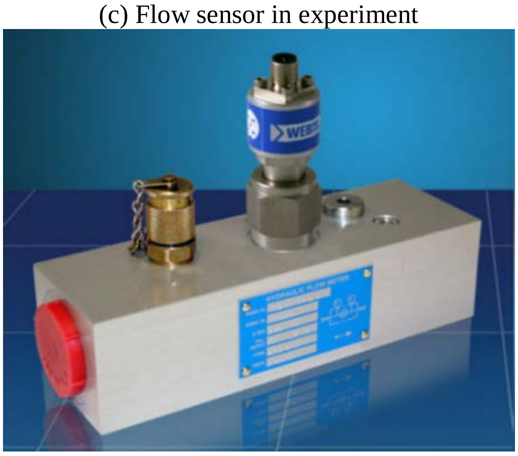

(d) LT1600 turbine flow meter

Fig.14. Outlet flow test experiment of piston pump

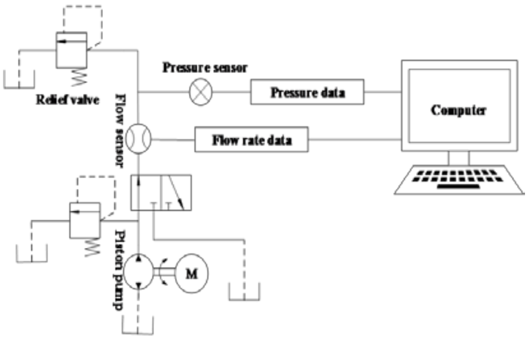

Fig.15. Diagram of the flow rate test experiment

The workload of different pressure load test is relatively large, the experiment is carried out with 100bar and 200bar pressure loads as examples. By comparing the simulation results with the experimental data, when the load pressure is respectively 100bar and 200bar the simulation data are consistent with the experiment data. The comparison results are shown in Fig.16, Fig.17 and Tab.10.

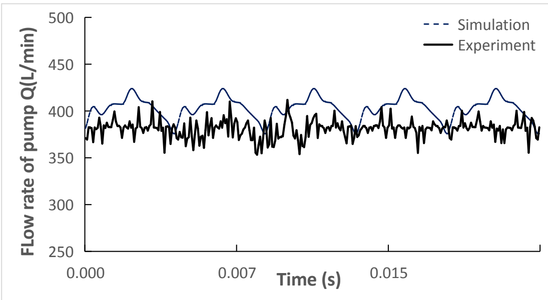

Fig.16. Simulation and experimental data under 100 bar load pressure.

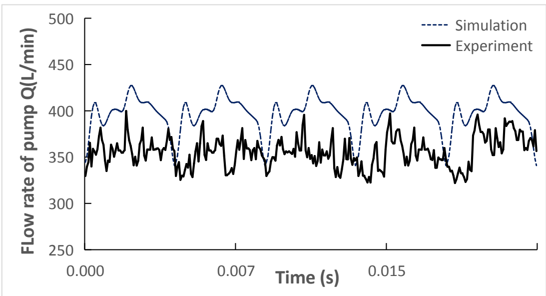

Fig.17. Simulation and experimental data under 200 bar load pressure.

Tab.10. Comparison of flow ripple rate of simulation and experiment.

Load (bar)	Type	Q_{max} (L/min)	Q_{min} (L/min)	Q_{ave} (L/min)	δ (%)
100	simulation	423.86	375.76	402.75	11.9
	experiment	406.82	360.26	385.79	12.1
200	simulation	427.29	340.90	396.81	21.8
	experiment	427.63	352.51	363.22	21.9

The above results demonstrate that the simulation data and the experimental data are consistent with each other under 100bar and 200bar load pressure, so the simulation data is correct.

CONCLUSIONS

In this study, the theoretical flow rate of PV270 type piston pump is calculated, and the simulation of piston pump with pre-compression chamber structure is conducted based on CFD with consideration of compressibility of oil in this paper, the piston pump outlet flow ripple are compared under different load pressures, different pump speeds and different pre-compression chamber structures. The results show that the flow ripple of piston pump is not only affected by the load pressure and pump speed, but also are affected by the damping hole diameter, damping hole span angle and volume of the pre-compression chamber. The load pressure has a great influence on the flow ripple of piston pump, while the pump speed has a little effect and can be ignored. Furthermore, when the damping hole diameter and damping hole span angle of the pre-compression chamber change from small to large in the setting interval, the flow ripple rate will present a minimum value. When the volume of the pre-compression chamber changes from small to large, the flow ripple will continue to decrease, although the volume change has little effect on the flow ripple when it reaches 500cm3.

The second order response surface function models with respect to the damping hole diameter and damping hole span angle of the pre-compression chamber are built based on DOE and approximate model methods. The damping hole diameter and damping hole span angle are optimized based on the response surface function model. Finally, flow test experiments are performed on the piston pump, with results demonstrating that the simulation and the experimental data are consistent with each other, specifically that the flow ripple rate is reduced when the load pressure is 100bar,200bar and 300bar, respectively.

ACKNOWLEDGMENT

Financial support for this work was provided by the National Natural Science Foundation of China and Natural Science Foundation of Jiangsu Province which numbers are respectively “51305049” and “BK20161193”. Authors also thank YEOSHEN Hydraulic Co., LTD for providing a PV270 piston pump and experiment condition.

REFERENCES

Edge, K. A., Wing, T.J., “Measurement of the fluid borne pressure ripple characteristics of hydraulic components”, Proceedings of institution of mechanical engineering, Part

B:Management and engineering manufacture, vol. 197, pp. 247-254, (1983).

Harrison, K., Edge, K. A., "Reduction of axial piston pump pressure ripple," Proceeding of the Institution of Mechanical Engineers, Part I: Journal of Systems and control Engineering, Vol. 214, pp.53-64, (2002).

Manring, N.D., "The discharge flow ripple of an axial piston swash plate type hydro static pump," J Dyn Syst Meas Control , vol.122, pp. 263-271, (2000).

Manring, N.D., "Valve plate design for an axial piston pump operating at low displacements," J Mech Des, Vol.125, pp200-207, (2003).

Mandal, N., Saha, R., Sanyal, D., "Theoretical simulation of ripples for different leading side groove volumes on manifolds in fixed displacement axial piston pump," Pro Inst Mech Eng I :J Syst Control Eng , Vol. 222(6),pp. 557-570, (2008).

Ma, J. E., Fang, Y. T., Xu, B., et al., "Optimization of cross angle based on the pumping dynamics mode," Journal of Zhejiang University,Vol.11(3), pp. 181-190, (2010).

Ma, J. E., Xu, B., Yang, H. Y., "Modeling and experiment study on fluid character of axial piston pump," Transactions of the Chinese Society for Agricultural Machinery, Vol. 41(1), pp. 188-194, (2010).

Yin, F. L., Nie, S. L., "Pre-compression angle of water hydraulic axial piston pump," Journal of Beijing University of Technology, Vol.41(9), pp. 1281-1288, (2015).

Wang, A. L., Wu, X. F., Ma, B., Zhou, C. L., "Dynamic response relationship between swash plate's structure parameters of piston pump and hydrodynamics features," Journal of Tongji University, Vol.39(4), pp. 586-590, (2011).

Wang, A. L., Wu, X. F., Zhou, C. L., Ma, B., "Multidisciplinary optimization of a hydraulic slide valve based on CFD," Journal of Shanghai Jiaotong University, Vol.44(12), pp. 1767-1772, (2014).

Chen, C. K., Wu, X. F., Hong, C. W., He, Y. F., "Flow ripple analysis and structural parametric design of a piston pump," Journal of Mechanical Science and Technology, Vol. 31(9) , pp. 245-254, (2017).

Kumar, S. J., Bergada, M., Watton, J., "Axial piston pump grooved slipper analysis by CFD simulation of three-dimensional NVS equation in cylindrical coordinates," Computers & Fluids, Vol.38, pp. 648-663, (2009).

Manring, N. D., Zhang, Y. H., "The improved volumetric efficiency of an axial piston pump utilizing a trapped volume design," Journal of Dynamic systems, Measurement and Control, Vol. 123(1), pp. 181-190, (2001).

Paolo,C., Andre, V., Germano, F., Gian, L. B., "Modelling of fluid properties in hydraulic positive displacement machines, " Simulation Modeling Practice and Theory , Vol.14, pp. 1059 -1072, (2006).

DING, H., VISSER, F. C., JIANG, Y., et al., "Demonstration and validation of a 3D CFD simulation tool predicting pump performance and cavitation for industrial applications," ASME Journal of Fluids Engineering, Vol. 133, pp. 011101, (2011).

Guan, C. B., Jiao, Z. X., "Dynamic optimization method for valve plate structure of aviation piston pump," Journal of Beijing University of Aeronautics and Astronautics, Vol. 37(3), pp. 274-278, (2013).

帶預壓縮結構的柱塞泵CFD模擬與實驗

吳小鋒 江煒
常州工學院機械與車輛學院

陳志鏗
國立台北科技大學車輛學系

洪智偉
油昇油壓機械公司

摘要：柱塞泵的柱塞腔吸完油經過配流盤預壓縮區域時會引起柱塞泵出口壓力和流量的脈動，從而產生柱塞泵內的流體雜訊。本文以某型號帶預壓縮腔結構的柱塞泵為物件，利用PUMPLINX對該柱塞泵內部流體進行了CFD模擬，結果顯示柱塞泵出口流量脈動受負載壓力、泵轉速以及預壓縮區腔結構的影響。借助於DOE實驗設計和近似回應面函數方法，獲得了在負載壓力分別為100bar、200bar、300bar情況下柱塞泵出口流量脈動率關於預壓縮腔阻尼孔跨度和直徑的二次回應面函數，並以流量脈動率最小為目標對結構進行了優化。最後，進行了該柱塞泵流量測試實驗，驗證了模擬結果的正確性。